

# EMCal calibration in preparation for QM 2002

Mickey Chiu<sup>a</sup>, Gabor David<sup>b</sup>, Justin Frantz<sup>a</sup>, Edward Kistenev<sup>b</sup>,  
Christian Klein-Bösing<sup>c</sup>, Saskia Mioduszewski<sup>b</sup>, Péter Tarján<sup>d</sup>,  
Hisayuki Torii<sup>e</sup>, Viktor Veszprémi<sup>f</sup>, Maxim Volkov<sup>g</sup>

July 12, 2002

<sup>a</sup> Columbia University, NY, USA

<sup>b</sup> Brookhaven National Laboratory, NY, USA

<sup>c</sup> Westfälische Wilhelms-Universität, Münster, Germany

<sup>d</sup> University of Debrecen, Hungary

<sup>e</sup> Kyoto University, Japan

<sup>f</sup> Florida Institute of Technology, FL, USA

(on leave from the University of Debrecen, Hungary)

<sup>g</sup> Kurchatov Institute, Moscow, Russia

## 1 Introduction

The PHENIX Electromagnetic Calorimeter (EMCal) consists of 8 sectors in two subsystems. The 6 lead–scintillator sectors of the calorimeter (often referred to as PbSc) have 64 layers of lead and scintillator sheets with longitudinal wavelength shifting fiber readout. The 2 lead glass sectors (PbGl) use the Cherenkov effect to measure the energy of relativistic particles. The EMCal was designed primarily to make precision measurements of promptly produced photons and electron pairs from nucleus–nucleus collisions at RHIC.

In the PHENIX Electromagnetic Calorimeter both the energy and the time of arrival of incoming particles are measured. The energy as well as the time response of the system had to be tuned as a prerequisite to the analyses for Quark Matter 2002. The calibration work (done mostly in the first half of 2002) is described in this analysis note.

## 2 Gains (Viktor Veszprémi)<sup>1</sup>

### 2.1 Time dependence

The ratio between an ADC count, which can be found in the PRDF files and the corresponding measured energy is called the system gain factor. The product of an ADC count and the respective gain of an EMC tower yields the energy deposited in that tower in an event. The code that performs this calculation is in

`$CVSROOT/offline/packages/emc-calib/Calib/emcRawDataCalibrator.C`, and is called by the PHENIX offline reconstruction software during DST production. The variation of gains is periodically monitored by a gain tracing system via measuring the energy of laser impulses of precisely known intensity. The intensities of the laser impulses are measured by photodiodes and are used as normalization factors to eliminate the intensity fluctuation. For monitoring the response of the electronics a certain amount of charge (a test pulse) is injected into it prior to the pre-amplifier, the reading of which serves as another normalization factor to compensate the fluctuation of the signal amplification in the electronics. The system gain is directly proportional to the product of these two correction factors.

Since gains are not measured every second, a set of them are fit by series of straight lines, and the instantaneous gain at any intermediate time between two measured points can be calculated using the parameters of the fit. These parameters are stored in the database but they also can be read in from plain text files (copies of which can be found under `/phenix/workarea/veszpv/gains*`). One file contains a gain set of one supermodule in the following format: channel number; time offset in seconds measured from the validity date of the set; intercept; and slope of the line. The time variation of intercepts is shown in Fig. 1. Here the gain factors are divided by the first set of those respectively to every channel.

A similar set of plots in Fig. 2 shows the run dependence (cf. time dependence) of the intercept of gains in different granules (sector pairs). Although it is possible to calculate the gains at any second of a run (using the slope of the line), that is not implemented in the data-calibrator code; therefore, only the intercepts shown on the plots are used by the offline reconstruction to get a single gain for every granule in every run.

---

<sup>1</sup>The people next to the section titles are those responsible for writing the section and

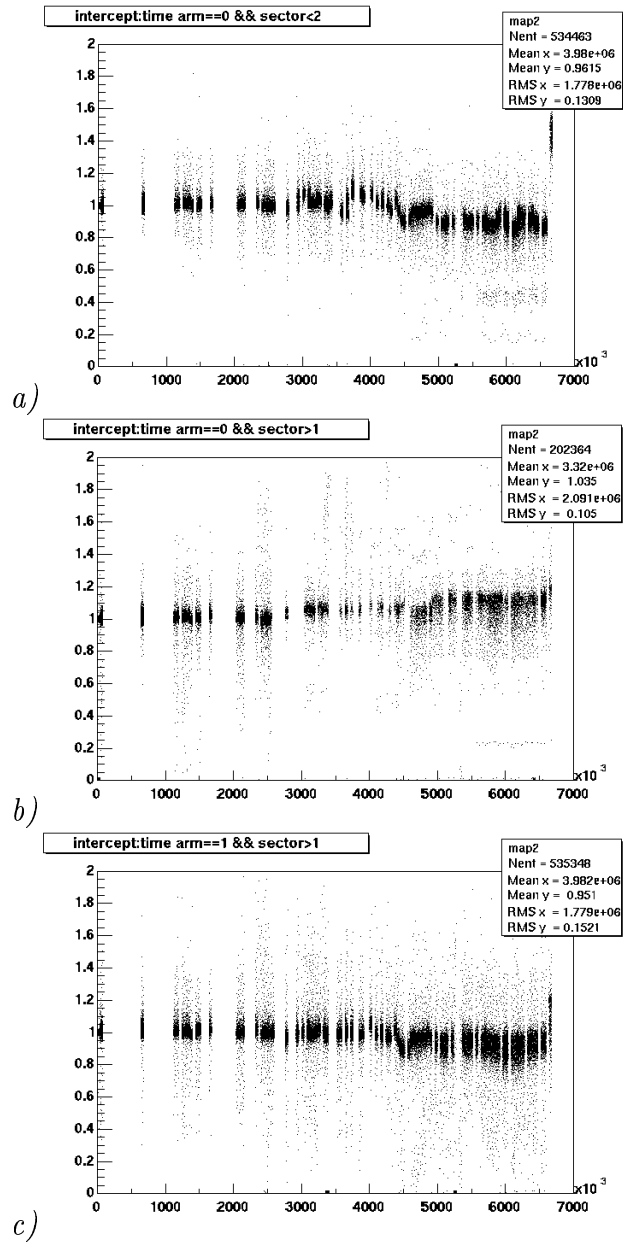
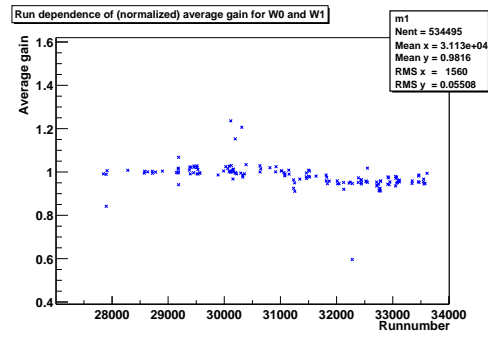
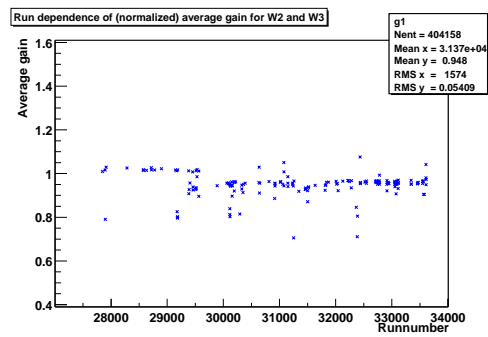


Figure 1: Time variation of gains in the 3 PbSc granules. *a)* Sectors W0 and W1; *b)* sectors W2 and W3; *c)* sectors E2 and E3. The horizontal axis shows time measured in seconds; gains are normalized to the gain in the first bin.

a)



b)



c)

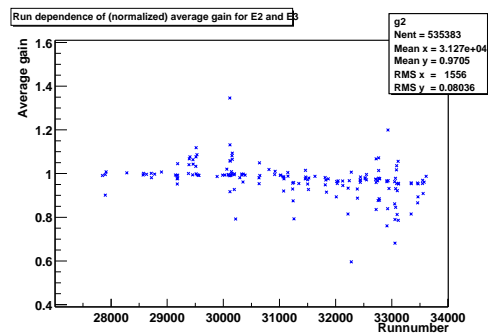


Figure 2: Run dependence of gains in the 3 PbSc granules. a) Sectors W0 and W1; b) sectors W2 and W3; c) sectors E2 and E3. Gains are normalized to the gain in the first bin.

## 2.2 Validity of gain sets

The gain set labelled Run2-1 is valid from Sept 10, 2001 to Oct 12, 2001. The gain files contain an entire set of gains for the existing supermodules at that time. (4 new supermodules were instrumented in W3 during the shutdown in early October, making a total of 14 [18 in all other PbSc sectors]).

Run2-2 is valid from Oct 12, 2001, and, with the exception of W2 and W3, gains remain unchanged from Run2-1.

## 2.3 Usage in Year-2 analysis

In the energy calibration of Year 2 data in preparation for QM2002 the gain tracing system was *not* used. For the entire period of Run-2 the first valid set of system gain factors was applied. This was decided due to the lack of knowledge on how the gain tracing worked and of sufficient statistics to investigate that. A part of the data was processed using the gain tracing, but no analysis cross-check (e.g. width and position of the  $\pi^0$  peak) gave acceptable results, thus the idea was temporarily abandoned.

The energy calibration (MIP peak position) was monitored with the Quality Assurance (QA) code and the acquired information was used to improve that in the microDST afterburner process (see Section 4).

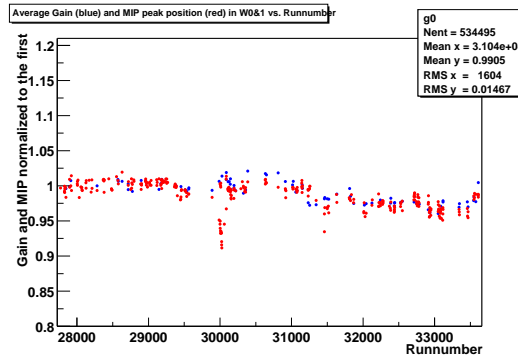
## 2.4 For near future studies

Fig. 3 displays both the average of the gains in the 3 PbSc granules (from the gain tracing, which was *not* used) and MIP peak positions against run numbers on arbitrary scale. (They were drawn like this so that both could be seen at the same time.) The plots imply a connection between the gains and the corresponding MIP peak.

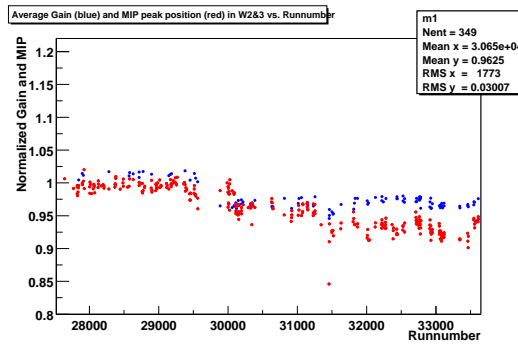
## 3 Timing (Péter Tarján)

In addition to the energy of the incoming particles, their time of arrival is also measured. The origin of the time scale is chosen to be the instant when photons coming from the interaction vertex hit the front face of the not the only ones who had worked on it. Their email addresses are listed in the appendix.

a)



b)



c)

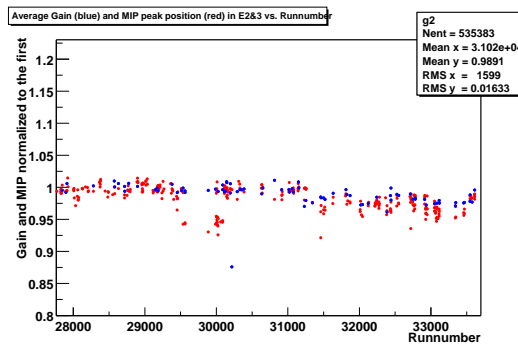


Figure 3: Correlation of gains (blue) and MIP peak positions (red) in the 3 PbSc granules. a) Sectors W0 and W1; b) sectors W2 and W3; c) sectors E2 and E3. Gains are normalized to the gain in the first bin.

calorimeter. In reality, the arrival time of photons has an offset, which has to be corrected. We applied two sets of corrections:

- global (i.e. run-independent) tower by tower corrections compensate the differences in the response time of individual channels (9216 in the PbGl part of EMCal, 15552 in PbSc, although some towers are not instrumented) thus reducing the width of the photon timing peak;
- sector-wide run by run corrections (8 numbers per run), which move the offset photon peak to 0.

### 3.1 Tower by tower corrections

Tower-by-tower corrections were produced independently by Hisayuki Torii and Edward Kistenev. Both of them divided the runs into pre-Oct 11 (runs starting with run 27808 but before run 29888) and post-Oct 11 runs (run 29888 and later). (Runs before run 27808 were not analyzed.) The reason for this division was that many calibration changes occurred during the shut-down around Oct 11 2001, which were clearly observable as a “jump” in the uncalibrated data. The photon peak widths in those two ranges had been dramatically different, as can be seen in Fig. 4. (This was also demonstrated in talks at the photon working group meetings as well as in the documentation of a Quality Assurance study of late April<sup>2</sup>. We think the reason behind this difference is that Hisa’s original set of tower by tower corrections, which were applied to all runs were produced from runs in the range 27808–29888 only.

A new set of corrections for post-Oct 11 runs from both Hisa and Edward were to resolve the problem. A sector by sector comparison of these two sets can be seen in Fig. 5, where the distributions of the differences of their respective correction factors were plotted. The two sets of corrections are not exactly on each other, there is a systematic difference between Edward’s and Hisa’s. The decision was finally made in favor of Edward’s set for he had reasonable corrections even for low statistics towers; when putting the numbers into the database, this systematic difference was taken into account.

For a description of how the tower by tower corrections were established, see Edward’s analysis note at

<http://www.phenix.bnl.gov/phenix/WWW/p/draft/kistenev/qm2002/qm2002.doc>

---

<sup>2</sup>See <https://www.phenix.bnl.gov/WWW/p/draft/ptarjan/QAstudy>

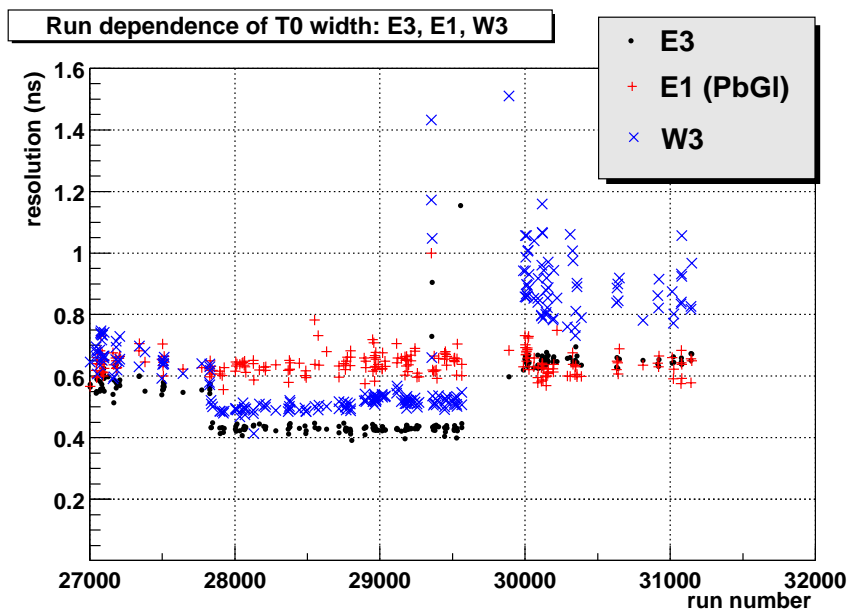


Figure 4: Photon peak width in the calorimeter *before* the afterburner in the best (E3) and the worst (W3) of the PbSc sectors and in one of the PbGI sectors (E1). Note the three regions with significantly different resolution in PbSc.

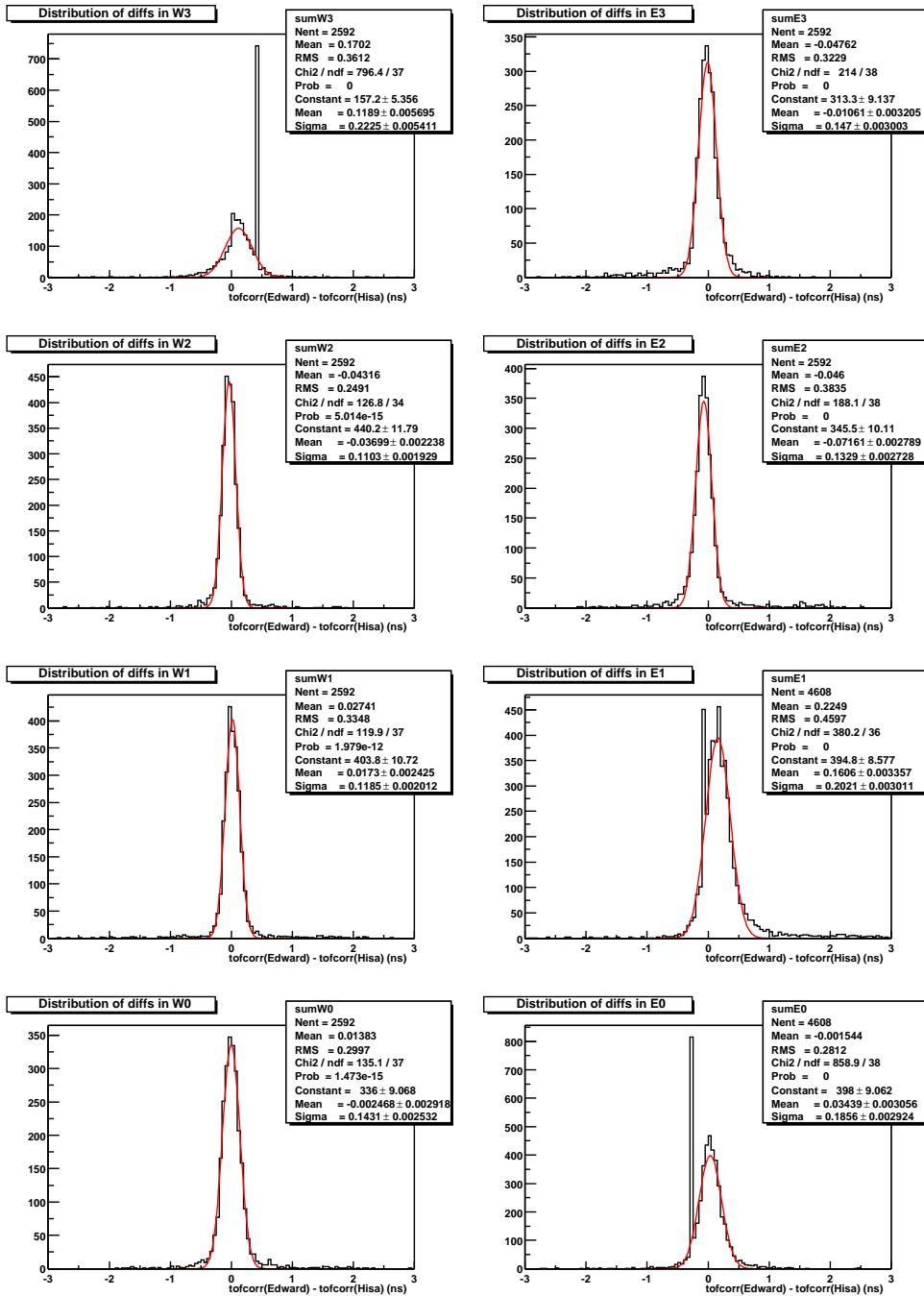


Figure 5: A sector by sector comparison of the tower by tower T0 corrections produced by Edward and Hisa.

## 3.2 Run by run corrections

Right before their deletion from disk (05/27/2002), all reasonable size v03 DST's ( $\approx 600$  files, 0000 segment of each run) were collected and the QA code `run2_ver7` was run on them. As far as timing goes, the QA output for the calorimeter contains histograms with the photon peak in each sector. Each histogram is then fit with a Gaussian around its maximum and those fit parameters are written into the QA summary file. As the ideal position of the peak is at zero, the offset gives the (additive) correction itself for that particular run and sector; the width of the fit is used to check the resolution of the calorimeter.

T0 offsets and timing widths were extracted from all QA summaries into a text file, and the text file was used to update the run by run corrections in the database. For the runs whose 0000 segment was broken (due to e.g. database access failure during production) or had low statistics, T0 offsets were determined from the microDST's.

While the afterburner pass was rolling, Tom Hemmick discovered a problem with the timing of sectors W2 and W3: plotting the  $m^2$  distribution in each sector (see Fig. 6a), he found that the proton peak in W2 and W3 is considerably lower than it should be (0.87 GeV<sup>2</sup>).

The issue was referred back to Edward who came up with some corrections to his correction: a universal scale factor of 0.956 to apply to each sector in every run, and an additional (multiplicative) factor of 1.267 for W2 and W3 in all runs after and including 29888. (Look for `hadronCorrFactor` in `$CVSROOT/offline/packages/afterBurner/EmcTofAfterBurnerV1.C.`)

The result of this additional tweaking is plotted in Fig. 6b – the problem is indeed gone.

As a result of all the corrections applied in the afterburner, the photon peak is generally within 100 ps of 0 and in the PbSc part of calorimeter has a sigma around (or better than) 400 ps, as shown in Fig. 7. Sector W3 is the worst of the PbSc sectors: it can at times be more than 200 ps off and have a resolution of 550 ps. The PbGl sectors have a resolution in the ballpark of 600 ps. In Fig. 8 the timing peak is plotted separately in each sector from an afterburned microDST.

An additional improvement over Year 1 data is that the photon peak now exhibits a Gaussian shape. This is demonstrated in Fig. 9, where the fraction of extracted  $\pi^0$ 's is plotted versus the width of the TOF cut for different  $p_T$  bins.

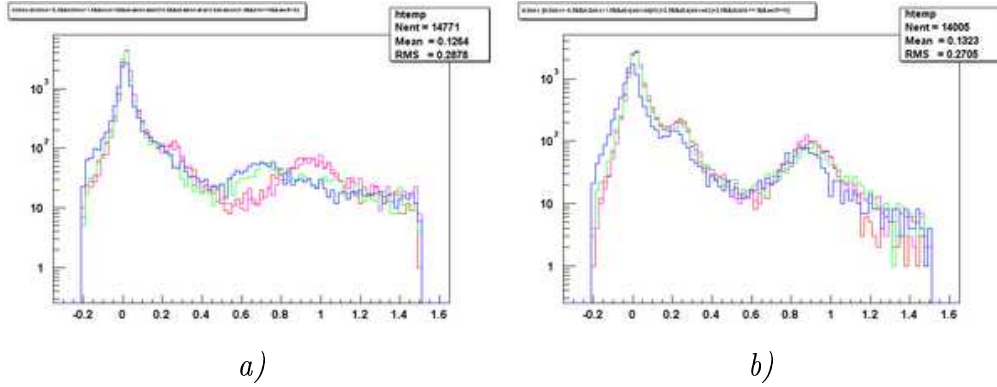


Figure 6:  $m^2$  distribution of West EMCAL sectors *a)* before and *b)* after the modified corrections. With the final corrections W2 and W3 are back in the company of the others. Legend: W0 = red; W1 = magenta; W2 = green; W3 = blue.

The used corrections are in the database with insert times no later than 06/17/2002.

### 3.3 Energy dependence (Viktor Veszprémi)

Although unlike Year 1, in Year 2 the timing is really Gaussian, there is a systematic shift in the timing peak position as a function of energy. This effect is qualitatively reproduced in the simulation, with the shift in the opposite direction.

There are three known possible sources of energy (momentum) dependence of the TOF measurement in EMCAL. One major source is the so called slewing effect, i.e. an energy dependent readout of the TDC coming from the fact that the readout is triggered by a certain signal level which is achieved earlier in case of signals of higher amplitudes (their slope is also steeper). Another source, which can cause similar effect, is the variation of depth of EMCAL showers. Light signals from deeper showers of higher energy reach the electronics faster than those from shallower ones. These two effects make the signals of higher energy recorded earlier. The correction for them was done by Edward Kistenev, obviously on lower statistics. Since now sufficiently high statistics exist in Year 2 data, it is going to be possible to study these effects reaching out to a wider range of cluster energy.

A third possible known effect can come from the cross talk of adjacent

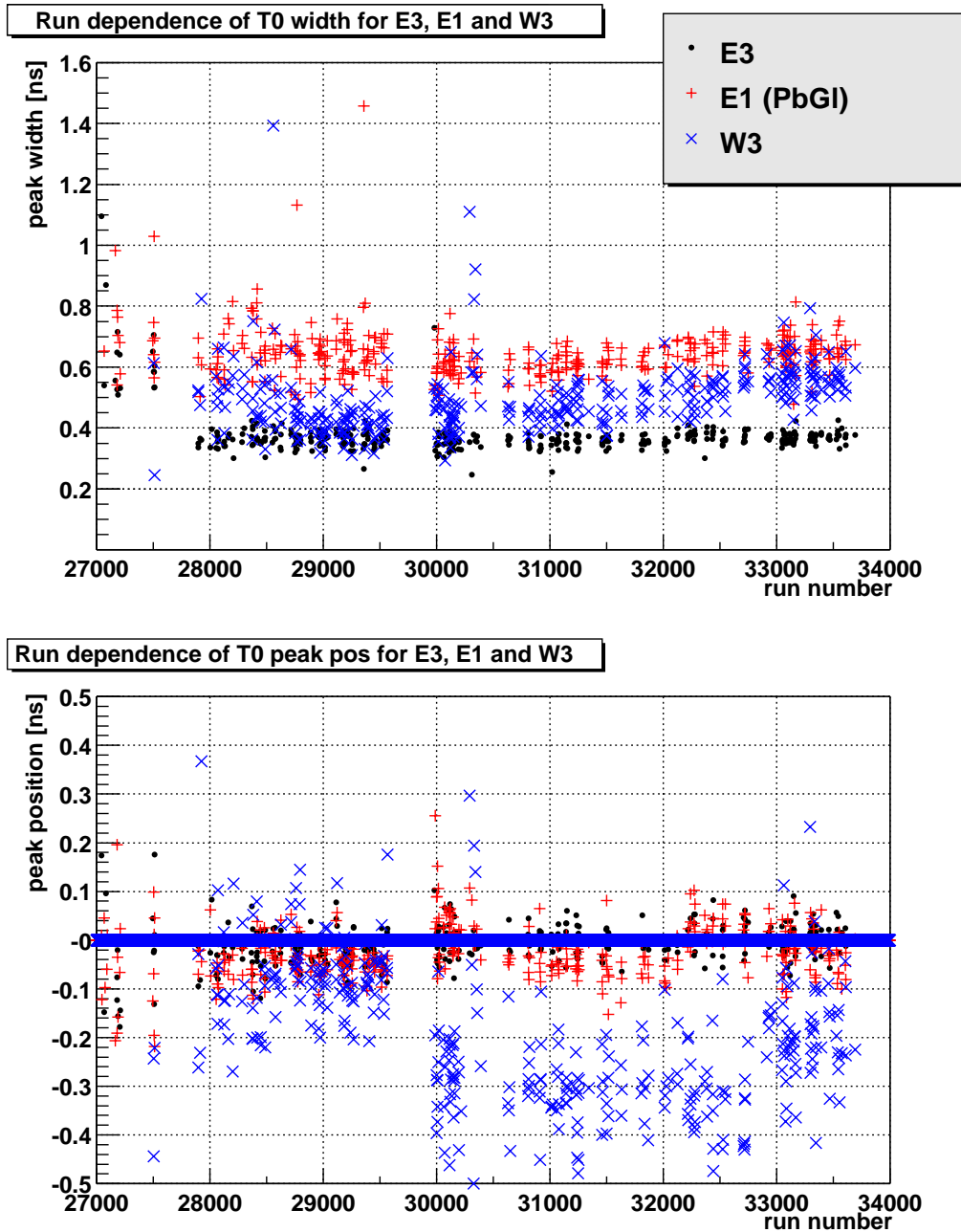


Figure 7: Photon peak width in the calorimeter *after* the afterburner in the best (E3) and the worst (W3) of the PbSc sectors and in one of the PbGI sectors (E1). Note that the three regions with different resolutions are gone.

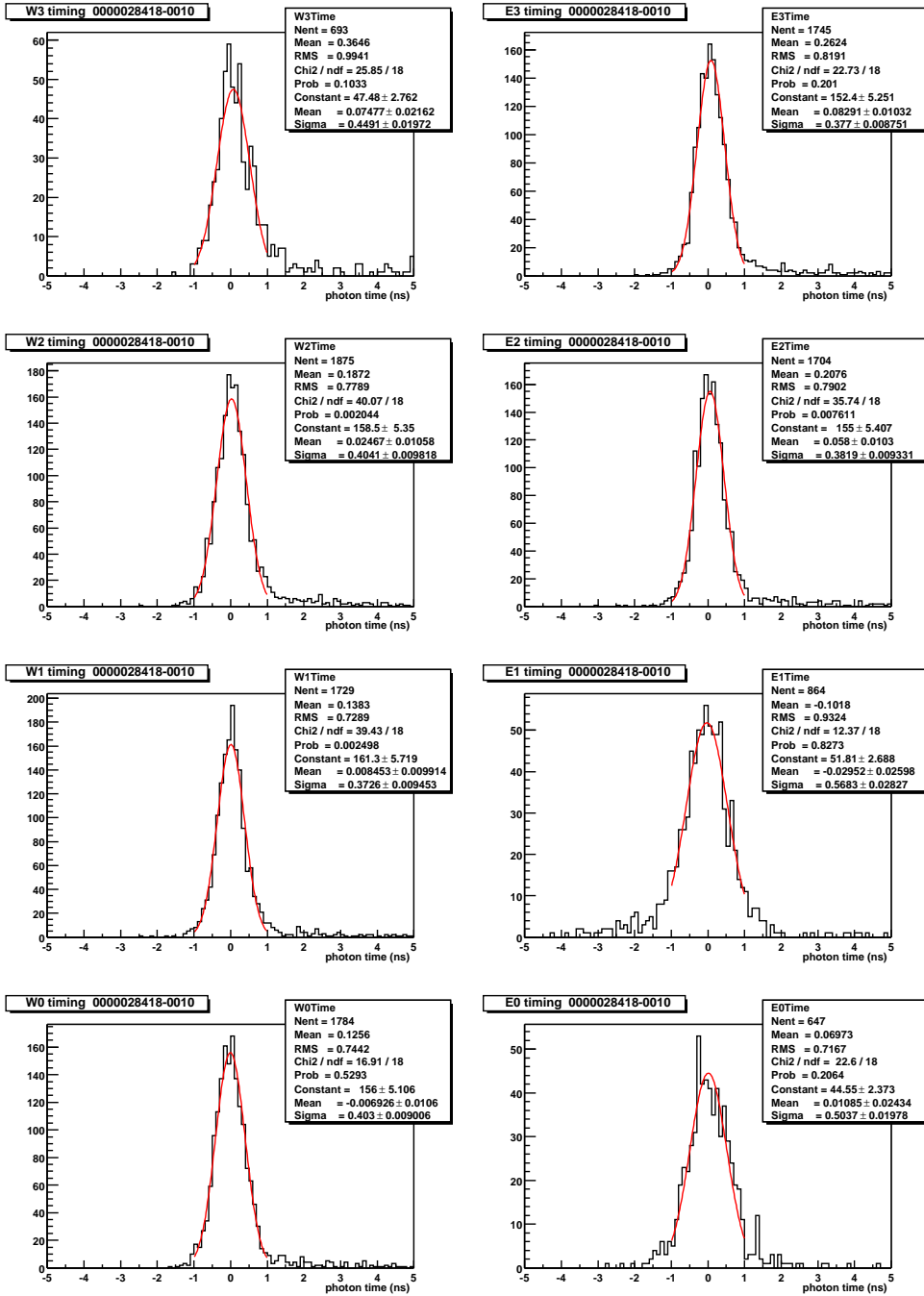


Figure 8: The photon peak in the calorimeter in run 28418 segment 0010.

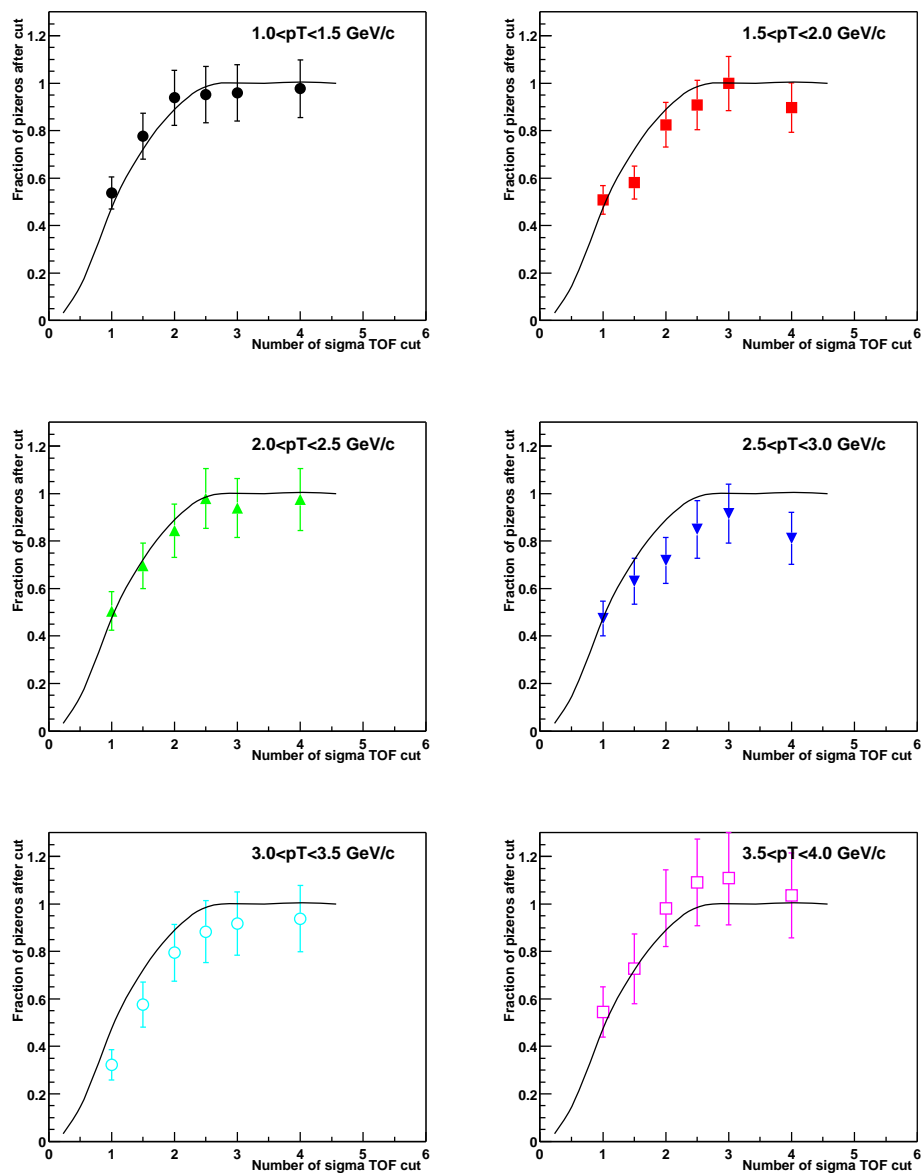


Figure 9: Fraction of counts extracted with TOF cut to counts extracted with no TOF cut vs the width of the TOF cut. Points are data, the continuous line is the theoretical value calculated from the Gaussian lineshape only. Data are consistent with the assumption of a Gaussian distribution.

channels in EMCal timing electronics.

For now, without explaining their cause, only the effects have been studied by applying a very simple cut on the HRD nanoDST's without explaining their cause. Taking advantage of that these nanoDST's already contain photons cluster-closest track associations, and that they have a higher yield of photons on higher energies, a considerably high statistics of clear photon-sample were collected.

The following cuts were applied:

- time of flight (BBC T0 subtracted) less than 3 ns
- closest track associated to a certain cluster should intercept EMCal at least 10.8 cm far along both indz and indy direction (practically  $dz > 10.8$  and  $d\phi > 0.02$ )
- photon-like shower shape:  $\chi^2 < 3.0$

The data was collected for PbSc and PbGl separately.

It seems that going to higher energies the photon arrival time, which was to be calibrated to 0, shifts upwards. This effect is the opposite of what we expect.

Nevertheless, this observed shift can result in an efficiency loss in any analysis that applies a cut on the EMCal TOF and does not take its energy (momentum) dependence into account. Not only are the photons affected, but also every other particle type, e.g. electrons, as Edward Kistenev's plots (Fig. 10) indicate.

For photons, the rate of shift and the change of sigma of the TOF distribution were calculated at various energy ranges (see Fig. 11). The results are shown in Table 1.

## 4 Energy (Viktor Veszprémi)

The final energy correction was performed in the `EmcEnergyAfterburner`, which can be found under `$CVSROOT/offline/packages/afterBurner`. The correction table of the scale factors used by the afterburner was based on an energy measurement of minimum ionizing particles by Edward Kistenev.

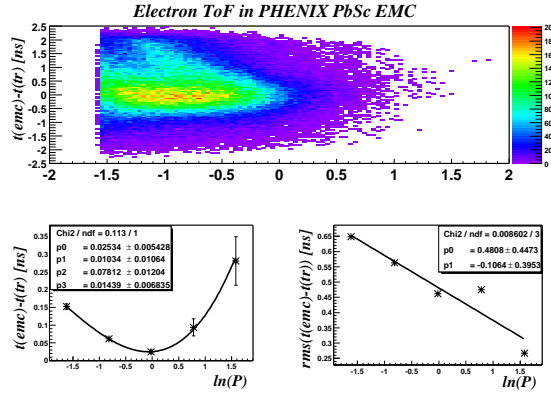


Figure 10: Top panel: difference between the time measured in the calorimeter and the expected time using tracking pathlength versus  $\ln(P)$  for identified electrons, where  $P$  is the momentum of the electron. Bottom left: mean values of the above distribution at different  $\ln P$  slices. Bottom right: RMS of the above distribution at different  $\ln P$  slices.

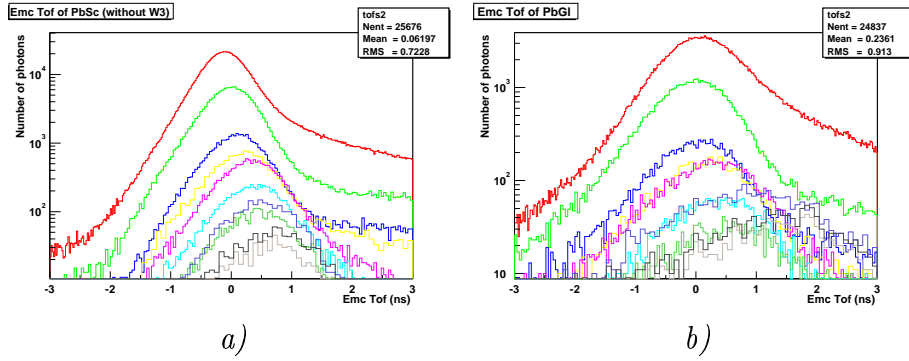


Figure 11: EMCal TOF in different energy bins in a) PbSc b) PbGl. The colors correspond to the energy bins in Table 1.

Table 1: Mean photon peak position and its  $\sigma$  as observed in PbSc data and PbGl data as a function of photon energy.

$E$ (GeV)	PbSc mean (ns)	PbSc $\sigma$ (ns)	PbGl mean (ns)	PbGl $\sigma$ (ns)
0.5–1.0	−0.107	0.35	0.09	0.62
1.0–1.5	−0.01	0.39	−0.33	0.60
1.5–2.0	0.1	0.43	0.13	0.65
2.0–2.5	0.21	0.48	0.18	0.72
2.5–3.0	0.32	0.50	0.3	0.7
3.0–3.5	0.38	0.52	0.34	0.77
3.5–4.0	0.38	0.54	0.5	0.85
4.0–5.0	0.45	0.54	0.84	1.1
5.0–6.0	0.6	0.6	1.44	0.94
5.0–10.0	0.7	0.6	1.4	1.0

The scale factors were calculated for each tower run– and time independently. One run independent scale factor was determined for each tower.

The scale factors were calculated such that they bring the MIP peak positions of all the towers to a common value; the towers that did not have a good MIP peak fit were corrected with a scale factor of their respective supermodule. This method is justified by the observed correlated behavior of towers in the same supermodule. Fig. 12 shows how the distribution of the scale factors looks in 3 sectors of the calorimeter. E0 is one of the two PbGl sectors, W0 is an example of the “good” PbSc sectors, whereas W3 is the worst of them on account of having a large number of hot and dead towers. The many outlying towers in the W3 tower energy scale factor distribution is one of the reasons why it is highly recommended to exclude W3 from every analysis.

## 4.1 Correction of towers in PbSc sectors

While testing the afterburner by looking at MIP peak positions and  $E/p$  ratios for electrons, an energy scale mismatch was revealed between different sectors and along three intervals of Run 2. This mismatch manifested itself in the MIP energies not being aligned in the different sectors with respect to each other and also in having sudden jumps around certain run numbers. This behavior was also observable in the QA output.

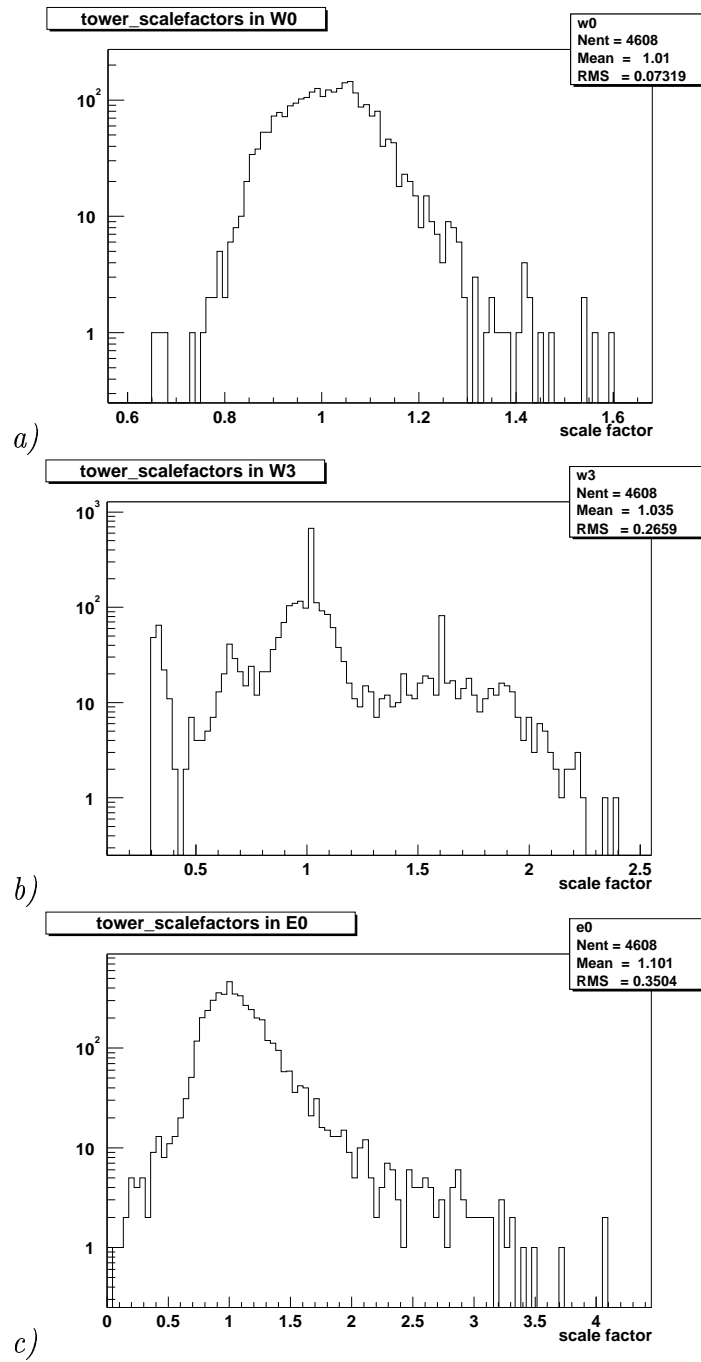


Figure 12: Distribution of scale factors as they appear on microDST's for *a)*, sector W0; *b)* sector W3 showing hot towers below 1 and partially dead towers above 1; *c)* sector E0 (PbGl)

Due to its problems the gain tracing system was turned OFF (see Section 2), and the pre-QM2002 calibration was done with constant, time-independent gains.

Based on the results of QA, the entire Run 2 was divided into three periods, and it was decided that for each period a separate correction table should be inserted into the database. Within each of these three periods a straight line of slope zero was fit to the run dependent MIP peak positions. The new corrections arose by multiplying the original tower by tower correction factors with the fit constants, thus creating 3 tables out of 1. As shown in Fig. 13*b*) the MIP peak in the middle period is about 2.5% lower in W2 and W3 than in the other sectors. For this reason those energies were multiplied by another factor to bring W2 and W3 in line with the rest of the PbSc.

The green points in Fig. 14 indicate that the energy scale has become consistent, and the expected run by run energy resolution is several percents.

The applied correction factors, after rescaling them so that the average MIP peak positions become equal can be found under

```
/phenix/u/veszpv/summary/ as  
tower_eScaleFactor_set1_x1.035_x1.025inW23.txt,  
tower_eScaleFactor_set2_x1.035_x1.025inW23.txt,  
tower_eScaleFactor_set3_x1.035_x1.025inW23.txt.
```

These correction factors are valid in the periods September 10 to October 16, October 16 to November 2 and from November 2 2001, respectively.

The result of the afterburner on limited statistics and the expected result of the  $\pi^0$  and  $E/p$  peaks were presented before the start of the full-scale official afterburner production.<sup>3</sup>

## 4.2 Correction of towers in PbGl sectors

Correction tables for the PbGl sectors provided by the PbGl group are also contained in the files mentioned above. The corrections are based on studies similar to those described in Subsection 4.1.

An independent cross-check of the energy calibration was done by Maxim Volkov, who studied the energy dependence of  $E/p$  ratio for electrons in both

---

<sup>3</sup>[http://www.phenix.bnl.gov/phenix/WWW/p/draft/veszpv/EmcEnergyAfterBurner/EMC\\_Energy\\_Afterburner\\_Status\\_Report.ppt](http://www.phenix.bnl.gov/phenix/WWW/p/draft/veszpv/EmcEnergyAfterBurner/EMC_Energy_Afterburner_Status_Report.ppt)

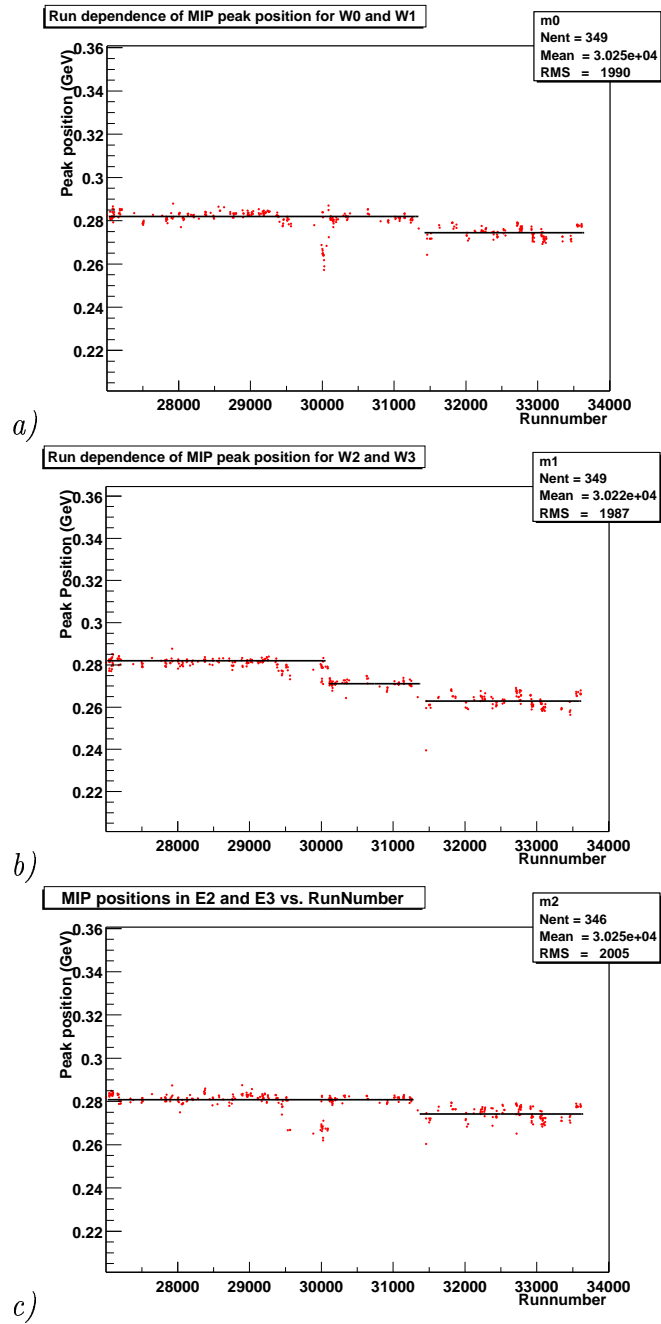
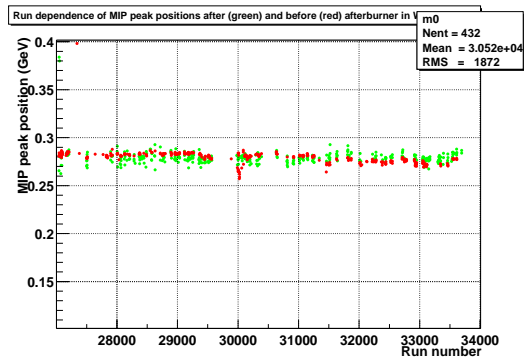
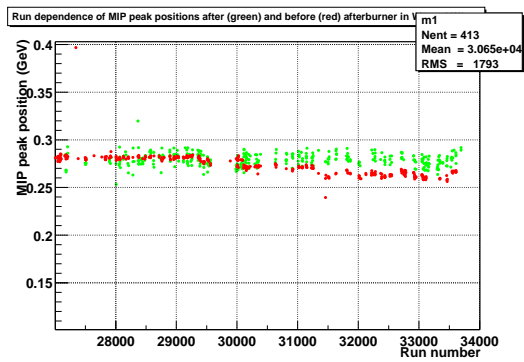


Figure 13: Run dependence of MIP peak positions in the 3 PbSc granules. *a)* Sectors W0 and W1; *b)* sectors W2 and W3; *c)* sectors E2 and E3.

a)



b)



c)

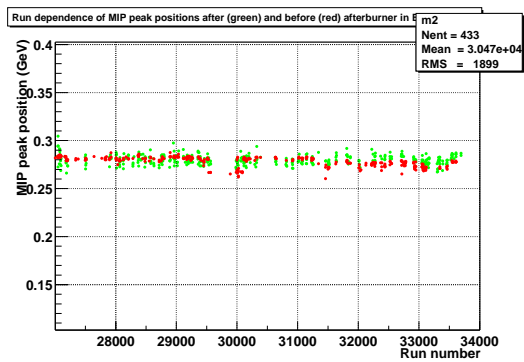


Figure 14: Fluctuation of MIP peak positions before (red) and after (green) the recalibration of the energy – as seen by the QA. a) Sectors W0 and W1; b) sectors W2 and W3; c) sectors E2 and E3.

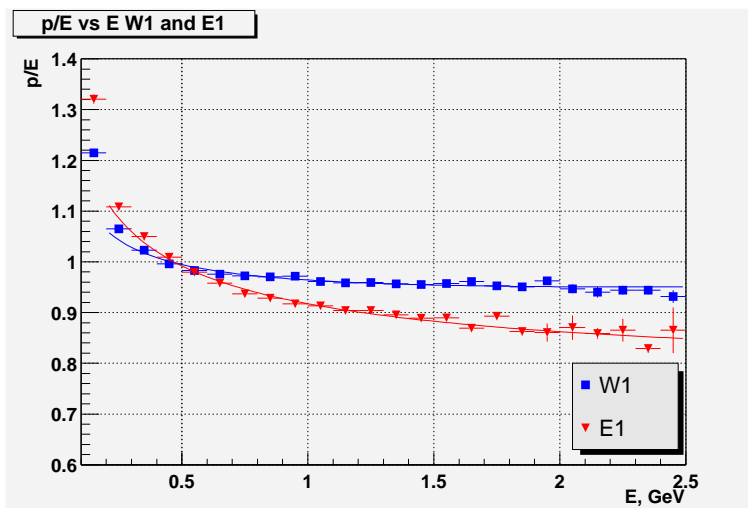


Figure 15: Maxim Volkov's study on the energy dependence of  $E/p$  ratios for electrons (06/10/2002).

PbGl and PbSc sectors. His results in Fig. 15 show the nice performance of PbSc as of June 10, 2002.

### 4.3 Consistency of energy spectra in PbSc sectors

Fig. 16 indicates the consistency of segment by segment energy measurements in different energy bins. This study was conducted to check whether we could see an expected 2% difference in photon energy spectra, when we compare those from photon converter runs to those from ordinary runs close to photon converter runs in time. During photon converter runs a cylindrical metal sheet was placed around and along the beam line. The thickness of the photon converter was such that approximately 2% of the photon yield was converted out without influencing the other particles and the background. In comparing a photon converter and a non-photon converter run, the background of the photon spectra were the same and the expected effect of interest were about 2%.

As Fig. 16 shows, even for selected runs the cluster energy spectra were not consistent enough to see a 2% difference.

The macros which selected 61 run segments out of 246, from which the

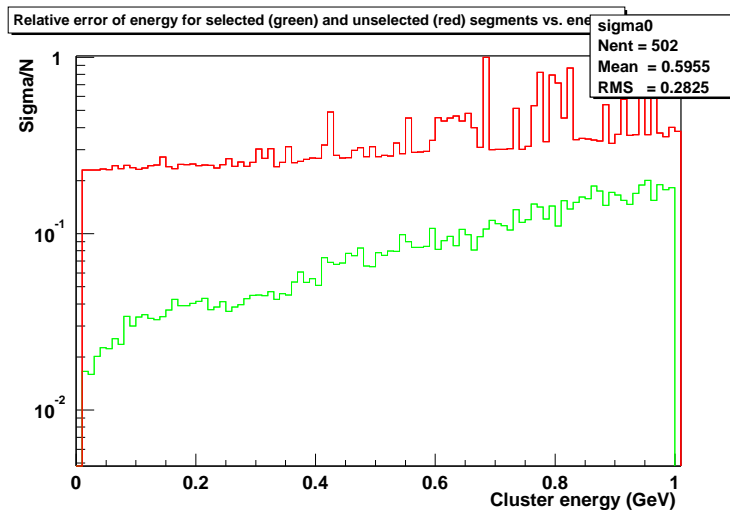


Figure 16: Statistical error of cluster energy spectra at each bin calculated for 246 segments (red) and 61 selected segments (green).

green graph in Fig. 16 was extracted are in  
[/phenix/u/veszpv/summary/run-selection](#).

The process happened in three steps. An ezdst application prepared the cluster energy spectra with the following cuts:

- cluster is in one of the 5 PbSc sectors;
- event is minimum bias;
- clusters containing dead or hot towers are excluded;
- 0-10% centrality.

In the second step a macro (`pass.C`) normalized the energy spectrum from each file dividing them by the number of clusters in the spectrum, calculated the statistical error bin by bin, and averaged the spectra coming from the different files.

In the third step another macro (`pass2.C`) selected those segments where the sum of the squared bin by bin deviations from the average energy spectrum was small enough. (The threshold was 0.0000021, where the number is measured on a scale where the integral of every cluster energy spectrum

is normalized to 1.0, and was chosen so that a not too small number of file segments get selected.)

As the results imply, in this year a photon analysis based on the photon converter is not feasible. In Year 3 the EMCal energy performance is expected to improve; however, using a photon converter with higher conversion rate would be advisable.

## 5 Hot/dead towers

### 5.1 PbSc EmCal Hot Tower Rejection (Justin Frantz)

The method for identifying hot towers in the PbSc EmCal sectors which were then added to the cluster warnmaps in the v03 microDSTs was a simple one based on hit frequency. The general method was as follows. First, on a run by run basis, the number of hits above a certain energy threshold were histogrammed for each tower. Second, again on a run by run basis for each of these thresholds, a histogram was made of the number of towers hit, and a Poisson or Gaussian was fit around the mean value. Third, one of the thresholds was chosen for each run, and all towers whose number of hits were above a certain number of standard deviations, defined by the fit function in the second step, were recorded for each run in text files based on the QA EMC extra reject list format. Last, the text files for all processed runs were combined into one large file containing the union of all identified hot towers. The EmcRejectAfterBurner code then updated the appropriate fields of all clusters based on this final list.

#### 5.1.1 Histogramming

On a run by run basis, the number of hits above a certain energy threshold were first histogrammed for each tower. Four thresholds were studied: 0 GeV (no threshold), 0.5 GeV, 1.0 GeV and 1.5 GeV. Fig. 17 shows an example of these histograms for run 30009.

#### 5.1.2 Fitting

For each of these thresholds, a histogram was made of the number of towers hit, and a Poisson and a Gaussian were fit around the mean value of number of towers hit. One other distribution was studied to use as fitting function: a

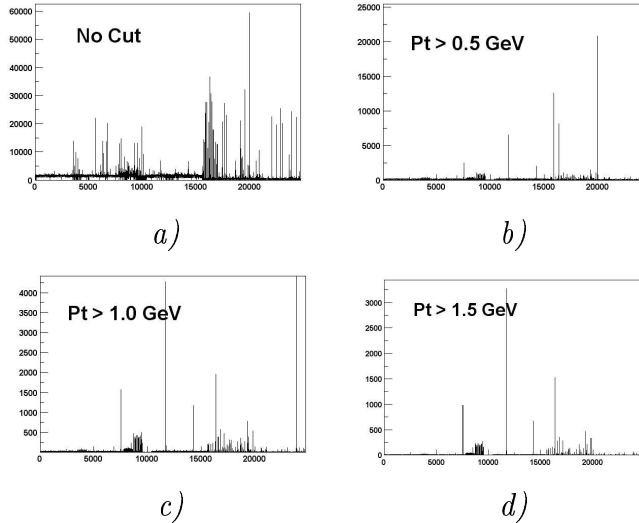


Figure 17: Number of hits vs EMCAL tower index with 4 different  $p_T$  cuts for run 30009.

binomial distribution, where the standard probability  $p$  and number of trials  $n$  and the scale factor were the fitted parameters. However this distribution was found generally not to have a significantly better  $\chi^2$  fit value, even for higher thresholds. Whether to use the Gaussian or Poisson results was decided upon run by run according to the  $\chi^2$ . In most cases, the results of the Gaussian fit were used. An example of the Gaussian fit is shown in Fig. 18.

### 5.1.3 Hot Tower Identification

Based on the results of the fit, a limit was chosen as the maximum number of hits a tower could have for the run and not be considered hot. All towers with number of hits above this limit would then be identified as hot. The limit and its definition were studied extensively: limits of 3–12 standard deviations (defined by the fitting functions or the raw RMS), as well as limits based on the statistics in a certain sample were studied and appropriate limits were chosen on a run by run basis. Four standard deviations was the value used most often. All towers with numbers of hits above the limit were written to files formatted according to the QA EMCAL extra reject list format. The processed runs included approximately 30% of the runs and 50–60% of the

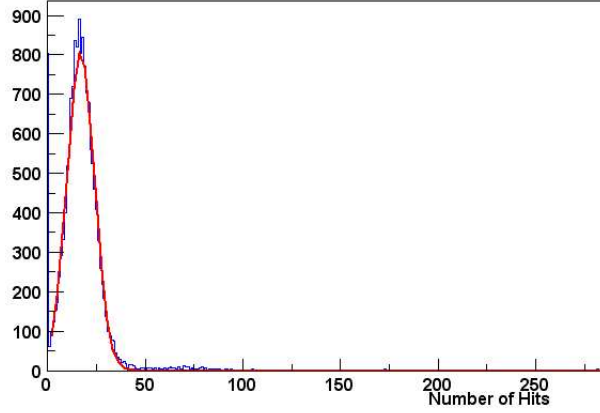


Figure 18: Gaussian fit to the distribution of number of hits with the cut  $p_T > 1.0$  GeV for run 30009.

v03 dataset. Then, for PbSc this run by run information was merged into a global (i.e. run-independent) reject list as follows. A tower was considered globally hot (and, consequently, made it into the global reject list) if it was hot in at least 10% of the runs processed. This conservative threshold still resulted in a relatively low number of hot towers outside W3, as shown in Table 2. The 5 good PbSc sectors have 26 hot towers (0.2%) out of a total of 12960.

Table 2: Number of hot towers in the PbSc reject list

sector	hot towers
W0	1
W1	12
W2	3
W3	400
E3	6
E2	4

#### 5.1.4 Afterburner

Finally, this single compiled list was combined with a PbGl list which included 52 PbGl hot towers (determined separately by the PbGl guys and not by our procedure) into a final single list stored in `/afs/rhic/phenix/-users/jfrantz/reject/reject.rej` and later in the afterburner database. The `EmcRejectAfterBurner` (`$CVSROOT/offline/packages/afterBurner/-EmcRejectAfterBurner.[Ch]`) marked the warnmap for PbSc (and warnmap and deadmap for PbGl) according to the tower map described in `$CVSROOT/-offline/packages/emc-calib/Calib/emcQAs.[Ch]` in all afterburned v03 microDST's. This was done by masking bits ON if they corresponded to one of our hot towers in a  $5 \times 5$  square (minus the corners) around the central tower (that with the highest energy deposit) in a cluster. This operation was irrespective as to whether the hot tower was actually included in the cluster or not, since this info is currently not available. (Except if the hot tower is the cluster center itself).

For PbSc, it was noticed that the deadmap and warnmap had been set to the same value for all runs in the DST's and the microDST's. Thus, to avoid destroying information, we cleared the cluster warnmaps and refilled them according to the hot towers we found. For PbGl, the warnmaps already contained information separate from the deadmap. Since Klaus Reygers had given the OK to mark the deadmaps, we simply added the 52 PbGl hot towers to the deadmaps of the PbGl Clusters, OR-ing bits such that the original deadmaps were left masked on.

#### 5.1.5 Results

An example for run 32123 is shown in Fig. 19 revealing the resulting improvement in the high energy cluster spectrum. Notice the dramatic reduction of the spectrum at high energies, which brings it in line with the expected exponential/power law drop off.

## 5.2 Deadmap/warnmap for PbGl (Maxim Volkov)

For the v03 DST production an extra reject list was created for the PbGl part of the calorimeter. This reject list contains 4 different flags for a tower (any non-zero value indicates trouble):

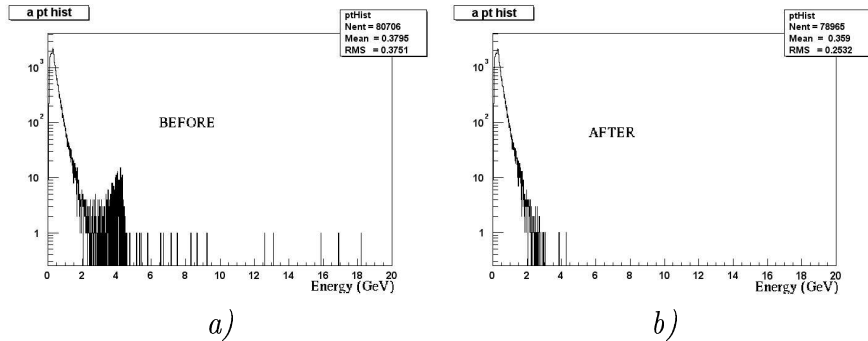


Figure 19: Energy spectrum *a)* before the hot tower removal; *b)* after the hot tower removal. Notice how the erroneous high energy tail of the distribution is gone.

1. **bad amplitude:** These towers are completely eliminated at the calibration stage by setting their gain to 0. These towers have absolutely crazy energy spectra that adversely affect the clustering procedure. All the clusters in the  $3 \times 3$  neighborhood should be rejected. Examples of amplitude spectra can be seen in Fig. 20.
2. **suspicious amplitude:** For the most part these are towers that are too noisy. They frequently have more than 0.2 GeV per event (for exact criteria and figures ask Christian <stevero@ikp.uni-muenster.de>). Another reason for declaring a tower suspicious was a bad Hi/Lo ratio (Fig. 21*b*, compare with *a*).
3. **bad TOF:** These were found based on TAC vs amplitude ADC spectra. Examples of good and bad TOF are shown in Fig. 22.
4. **suspicious TOF:** Introduced for symmetry reasons; analogous to “suspicious amplitude”. Not particularly useful at the moment.

Flags 2), 3), and 4) affect neither the calibration nor the reconstruction. These flags are just propagated to the warnmap (2 and 4) and deadmap (1 and 3) of neighbors for each tower (and cluster) that we write to DST’s. They can be used at the analysis stage, e.g. one could exclude all clusters in the  $3 \times 3$  area around a suspicious tower, or just exclude the cluster centered on this tower to save acceptance.

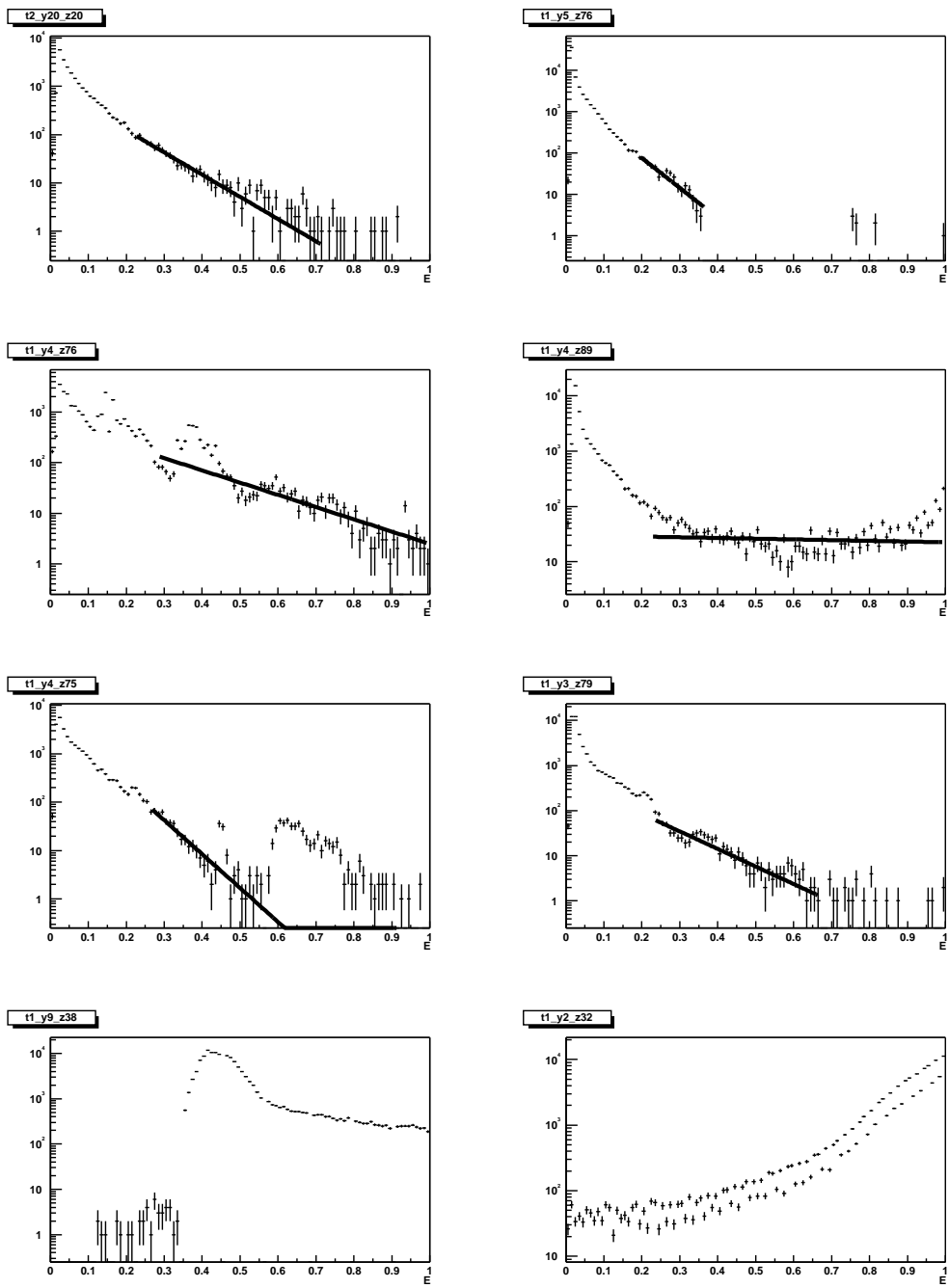


Figure 20: Upper left: a good tower amplitude spectra. The rest of the plots show one or another kind of deviation.

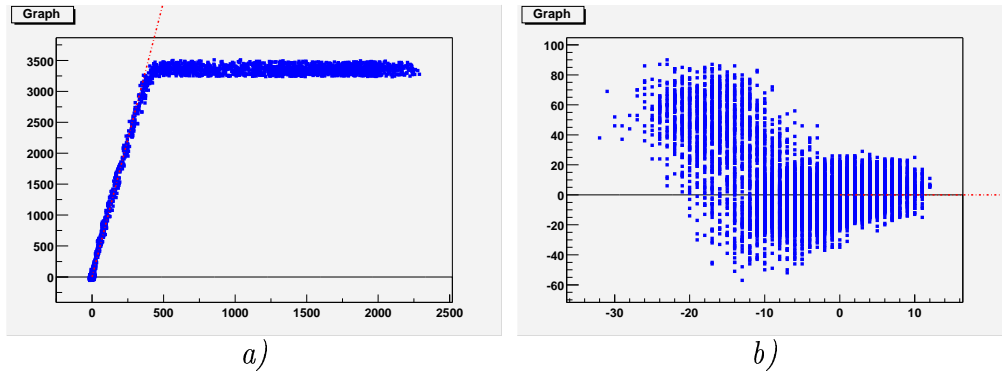


Figure 21: *a)* A good Hi vs Low gain spectrum. *b)* A bad Hi vs Low gain spectrum.

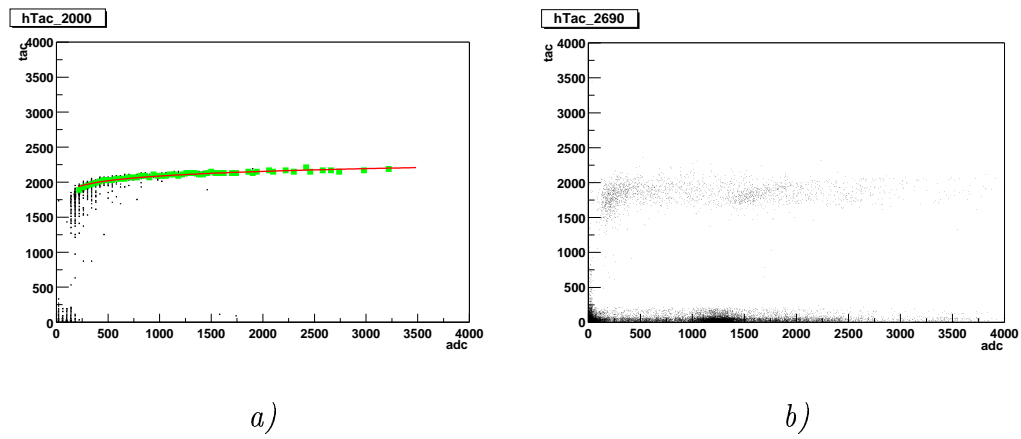


Figure 22: *a)* A good TAC vs ADC spectrum. *b)* A bad TAC vs ADC spectrum.

## 6 QA status (Péter Tarján)

Once the afterburning pass `burn1` had finished, we ran our QA macro on all afterburned nanoDST's, producing a QA histogram file and a QA summary file for each. The QA histogram files contain 8 timing histograms (one for each sector) and 3 energy histograms for the pairs of PbSc sectors (W01, W23, E23).

A relatively clean sample of photons went into the timing histograms; we only kept clusters meeting the following requirements:

- cluster energy > 0.5 GeV (`e>0.5`);
- photon probability > 0.1 (`prob_photon>0.1`);
- no dead or hot towers in the cluster (`deadmap==0 && warnmap==0`);

The energy histograms were filled with clusters from minimum ionizing particles that had:

- a matching charged track (`emctrkdz<5 && abs(emctrkdphi)<0.03`);
- cluster energy > 0.17 GeV (`e>0.17`);
- a shower shape not resembling that of a photon (`chi2>0.1 || twrhit<2`);

The positions, widths and fit parameters of the photon timing peak and the MIP peak were then extracted into the QA summary file.

Looking at this kind of information it had been quite clear at an early stage that W3 had serious problems:

1. W3 is not fully instrumented. That means that before October 11 only 10 supermodules were working out of 18. Then an additional 4 were instrumented, making a total of 14. This fact not only dramatically lowers its acceptance (especially for the pair measurements) but also makes acceptance calculations more complicated.
2. As W3 was instrumented last, it has the most faulty electronics board of all sectors, which also shows in its timing: its performance is significantly worse than those of the other 5 PbSc sectors.
3. W3 has literally hundreds of hot towers, much more than the rest of the PbSc sectors combined.

Table 3: Definition of the calorimeter status words

status word	meaning
-1	no QA status is set
0	run is good
1	run is bad
2	use at your own risk: bad timing
3	more dead towers in W3 than usual

Therefore it was decided to exclude W3 from every analysis wherever timing is an issue.

As after the afterburner corrections the energy calibration seemed to be in quite a good shape (with the MIP peaks being stable and at the same level in all sectors), the decision what status word individual runs should get was based on the timing information. The basic scheme can be seen in Table 3.

We divided the EMCal into 3 logically different parts with different status words: PbSc West, PbSc East and PbGl. Lists of runs meeting specific QA requirements can be assembled with the `runQuery` utility written by Saskia, e.g.:

```
runQuery --type=PHYSICS --field=1.0 --species=197 \
  --PBSCW=0 --PBSCE=0 --BBC=0
```

lists all full field physics Au–Au runs where all of the PbSc *and* the BBC is considered good. Status of individual runs can be queried with the `getStatus` utility.

The status words for the 3 calorimeter parts were set as follows:

- **status=0**: there are no known problems with the run.
- **status=1**: currently there are no runs with PBSCW=1 or PBSCE=1, the reason being that even if the timing is bad, the run may still be perfect for analyses only using EMCal energy. PBGL=1 results in a list of 10 runs in the range 30000-30019.
- **status=2**: for PbSc this means that a considerable fraction of the run had a photon peak more than 0.2 ns off zero *or* with  $\sigma > 0.6$  ns in any of the 5 “good” PbSc sectors. PBGL=2 returns no runs.

- **status=3**: only applicable to PBSCW – it means that there was a higher than usual number of dead towers in W3, but all other sectors looked fine.

As of today (06/28/2002), there are 278 runs in the database that have a status word of 0 for all 3 EMCal parts, 119 with PBSCW=2, 91 with PBSCE=2, of which 87 have status=2 for both. 17 runs (including those with PBGL=1) between runs 30000 and 30089 were marked with status=3. The 278 good runs were the following:

27000 27002 27044 27046 27048 27050 27052 27068 27074 28170 28199 28209  
 28212 28282 28367 28371 28375 28377 28379 28381 28444 27082 27094 27097  
 27497 28483 28488 28490 28573 28579 28632 28717 28718 28751 28775 28761  
 28765 28768 28795 28798 28902 28961 28962 28966 28968 28971 28972 28973  
 29014 29016 29017 29035 29036 29114 29116 29122 29146 29171 29178 29179  
 29184 29185 29186 29190 29197 29212 29213 29255 29256 29268 29362 29368  
 29372 29392 29380 29386 29404 29445 29451 29454 29459 29461 29510 29512  
 29514 29515 29531 29534 29562 29563 30112 30113 30114 30116 30117 30119  
 30123 30128 30143 30145 30146 30148 30153 30157 30158 30159 30193 30195  
 30197 30292 30328 30329 30344 30350 30356 30358 30388 30631 30633 30637  
 30642 30650 30807 30812 30813 30814 30816 30820 30910 30911 30913 30917  
 30920 30921 31009 31013 31014 31020 31024 31025 31058 31060 31072 31075  
 31076 31079 31080 31140 31142 31143 31145 31147 31148 31152 31230 31232  
 31233 31239 31240 31243 31244 31249 31252 31254 31256 31343 31459 31460  
 31463 31464 31500 31501 31515 31520 31628 31631 31633 31807 31811 31815  
 31824 31868 31831 31870 31836 32010 32011 32017 32028 32043 32123 32128  
 32217 32218 32221 32222 32239 32241 32242 32271 32272 32275 32279 32280  
 32382 32387 32435 32437 32438 32440 32441 32523 32525 32719 32720 32526  
 32548 32549 32709 32713 32716 32721 32722 32747 32748 32757 32761 32762  
 32763 32765 32766 32774 32776 32777 32780 32781 32782 32912 32913 32914  
 32925 32927 32928 32929 32932 32933 32934 32947 32948 32949 33049 33050  
 33051 33055 33056 33064 33068 33069 33077 33078 33082 33083 33085 33086  
 33116 33117 33458 33343 33345 33347 33467 33547 33557 33567 33608 33609  
 33611 33612

## 7 Evolution of the calibration and reconstruction code (Gabor David)

There were substantial changes in the calibration and reconstruction code with respect to the (final) Year 1 v05 scan. These are reflected in a completely new version of the calibrator (`emcRawDataCalibratorV1.C`) and the changes in the `$CVSROOT/offline/packages/emc-calib` directory tree.

Text files needed for data processing (including the “configuration file”) have been moved into the database, and fetching them from the database is now the default. However, for test purposes they can still be read from ASCII files by explicitly defining the corresponding source as `kFile_ASCII`.

The front end of the calibrator has been modified to accept the new (zero-suppressed) data, taken in the second half of Year 2 run. Also, the standard calibrator can now be used to process simulated PRDF’s as well.

In Year 2 both PbSc and PbGl used the Leading Edge Discriminator timing (as opposed to the derivative zero crossing of Year 1). The necessary slewing correction is now done inside the calibrator and the data on the DST are already slewing corrected (both in `dEmcCalibTower` and `dEmcClusterLocalExt`). Note that the applied slewing correction is “photon-specific”, while earlier testbeam results and current analyses of identified hadrons suggest that it will have to be modified for hadrons.

Also, the T0 in each channel is now determined from the physics data (instead of being tied to the laser, as in Year 1). As a consequence,  $t = 0$  for each channel is now defined as the mean arrival time of a photon from a  $z = 0$  vertex event to the front face of the respective tower (“nominal flashtime”). This flashtime subtraction happens in the calibrator (using the actual geometry, but without taking into account the actual event vertex). Therefore, we introduced a correction in the clustering (`mEmcClusterNewModule.C`). We first add the nominal flashtime (i.e. the one with  $z = 0$ ), then re-calculate it using the actual event vertex, and subtract this “actual flashtime”. Also, for Year 2 the event vertex is taken from the `VtxOut` class (by `mEmcRealEventModule.C`).

A new class (`PbScTimingFixes`) has been introduced to adjust for the channel by channel differences of timing within an FEM.

We fixed several bugs, including one that prevented the calibrator from actually applying the time-dependent gains, even if they were meant to be applied. It should be noted that all Year 1 scans (including the final Year 1 v05 scan) had this bug; therefore, gain tracing was not functional in Year 1

data.

A warnmap has been introduced for the towers (and propagated into the clusters); its definition is described elsewhere in this note.

## A People

The people contributing to the calibration work and to writing this analysis note were the following:

- Mickey Chiu <chiu@nevis1.nevis.columbia.edu>
- Gabor David <david@bnl.gov>
- Justin Frantz <jfrantz@nevis1.nevis.columbia.edu>
- Edward Kistenev <kistenev@bnl.gov>
- Christian Klein-Bösing <stevero@ikp.uni-muenster.de>
- Saskia Mioduszewski <saskia@bnl.gov>
- Péter Tarján <ptarjan@bnl.gov>
- Hisayuki Torii <htorii@bnl.gov>
- Viktor Veszprémi <veszpv@bnl.gov>
- Maxim Volkov <volkov@vskur4.mbslab.kiae.ru>